submitted to *Geophys. J. Int.*

Magnetic data radial inversion for 3-D source geometry estimation

L.B. Vital[1⋆]

[1] *Observatório Nacional, Gal. José Cristino, 77, São Cristóvão, Rio de Janeiro, 20921-400, Brazil*

Key words: Numerical solutions; Inverse theory; Magnetic anomalies.

⋆ Observatório Ncional, ON

1 METHODOLOGY

1.1 Forward problem

Let $\mathbf{d}^o$ be the observed data, whose ith element d_i^o, $i = 1, \ldots, N$, is the total-field anomaly produced by a 3-D source (Fig. 1a) at the point (x_i, y_i, z_i) of a Cartesian coordinate system with x, y and z axes pointing to north, east and down, respectively. We assume that the direction of the total magnetization vector of the source is constant and known.

We approximate the volume of the source by a set of L vertically juxtaposed 3-D prisms (Fig. 1b) by following the same approach of Oliveira Jr. et al. (2011) and Oliveira Jr. & Barbosa (2013).

The depth-to-the-top of the shallowest prism is defined by z_0 and we consider that the magnetization vector of all prisms has an intensity m_0 and a constant and known direction.

The horizontal cross-section of each prism is described by an arbitrary and unknown polygon with a fixed number V of vertices equally spaced from 0° to 360°, which are described in polar coordinates referred to an internal origin O^k .

The radii of the vertices (r_j^k, $j = 1, \ldots, V$, $k = 1, \ldots, L$), the horizontal coordinates (x_0^k and y_0^k, $k = 1, \ldots, L$) of the origins O^k, $k = 1, \ldots, L$, and the depth extent dz of the L vertically stacked prisms forming the ensemble are arranged in a M-dimensional vector $\mathbf{p}$, $M = L(V + 2) + 1$, given by

$$\mathbf{p} = \begin{bmatrix} r_1^1 & \ldots & r_V^1 & x_0^1 & y_0^1 & \ldots & r_1^L & \ldots & r_V^L & x_0^L \\ y_0^L & dz & & & & & & & & \end{bmatrix}^\mathsf{T}, \tag{1}$$

which will be estimated from the total-field anomaly data set.

The predicted total-field anomaly produced by the ensemble of L vertically stacked 3-D prisms is the sum of the magnetic effect of each prism at the ith observation point (x_i, y_i, z_i)

$$d_i(\mathbf{p}) \equiv \sum_{k=1}^{L} f_i^k(\mathbf{r}^k, x_0^k, y_0^k, \boldsymbol{\theta}, \mathbf{m}^k, z_1^k, dz), \quad i = 1, \ldots, N, \tag{2}$$

where $\mathbf{r}^k$ and $\boldsymbol{\theta}$ are the V-dimensional vectors containing the polar coordinates of the vertices of the kth prism whose the jth components are r_j^k and $\theta_j = (j-1)2\pi/V$, $j = 1, \ldots, V$, $k = 1, \ldots, L$, respectively. Additionally, $\mathbf{m}^k$ is the magnetization vector of the kth prism P^k, whose depth to the top is given by $z_1^k = z_0 + (k-1)dz$. We calculated the predicted total-field anomaly produced by the kth prism P^k, at the ith observation point (x_i, y_i, z_i), by using the Python package Fatiando a Terra (Uieda et al. 2013), which computes the non-linear function $f_i^k(\mathbf{r}^k, x_0^k, y_0^k, \boldsymbol{\theta}, \mathbf{m}^k, z_1^k, dz)$ based on the formulas proposed by Plouff (1976).

1.2 Inverse problem

The non-linear inversion of the total field anomaly consists in estimating the parameter vector $\mathbf{p}$ that minimizes the constrained objective function given by

$$\Gamma(\mathbf{p}) = \phi(\mathbf{p}) + \sum_{\ell=1}^{7} \alpha_\ell \varphi_\ell(\mathbf{p}), \tag{3}$$

subject to

$$p_n^{min} < p_n < p_n^{max}, \quad n = 1, \ldots, M, \tag{4}$$

where p_n^{min} and p_n^{max} are the lower and upper limits for the nth element p_n of the parameter vector $\mathbf{p}$, $\varphi(\mathbf{p})$ is the data-misfit function given by

$$\phi(\mathbf{p}) = \frac{1}{N}[\mathbf{d}^o - \mathbf{d}(\mathbf{p})]^2, \tag{5}$$

where $\mathbf{d}(\mathbf{p})$ is a N-dimensional vector whose the ith element d_i is the predicted total-field anomaly (equation 2) at the position (x_i, y_i, z_i), $i = 1, \ldots, N$.

The limits for the radii of all vertices of all prisms ($r_j^k, j = 1, \ldots, V, k = 1, \ldots, L$), the horizontal Cartesian coordinates of all arbitrary origins (x_0^k , y_0^k , $k = 1, \ldots, L$), and the depth extent of all prisms dz represented by p_n^{min} and p_n^{max} in the inequality constraints (equation 4) are defined by the interpreter element by element based on both the horizontal extent of the magnetic anomaly and the knowledge about the source.

To estimate a stable solution, we introduced a set of seven constraints on the geometry of the source. The ℓth constraint ($\ell = 1, \ldots, 7$) is represented by the function $\phi_\ell(\mathbf{p})$ (equation 3), where α_ℓ is a positive scalar representing its weight. We use the Marquadt's method to minimize the objective function $\Gamma(\mathbf{p})$ (equation 3) and introduce the inequality constraints (equation 4) by using a strategy similar to that presented by Barbosa et al. (1999). Our method imposes the constraints:

(i) Smoothness constraint on the adjacent radii defining the horizontal section of each vertical prism. This constraint imposes that adjacent radii within each prism must be close to each other. It forces the estimated prism to be approximately cylindrical. The matrix form of the this constraint is given by

$$\varphi_1(\mathbf{p}) = \mathbf{p}^\mathsf{T} \mathbf{R}_1^\mathsf{T} \mathbf{R}_1 \mathbf{p}, \tag{6}$$

where

$$\mathbf{R}_1 = \begin{bmatrix} \mathbf{R}^\sharp & \mathbf{0}^\sharp & \mathbf{0}^\sharp & \cdots & \mathbf{0}^\sharp & \mathbf{0} \\ \mathbf{0}^\sharp & \mathbf{R}^\sharp & \mathbf{0}^\sharp & \cdots & \mathbf{0}^\sharp & \mathbf{0} \\ \mathbf{0}^\sharp & \mathbf{0}^\sharp & \ddots & & \mathbf{0}^\sharp & \mathbf{0} \\ \vdots & \vdots & & \ddots & \vdots & \vdots \\ \mathbf{0}^\sharp & \mathbf{0}^\sharp & \cdots & \cdots & \mathbf{R}^\sharp & \mathbf{0} \end{bmatrix}_{VL \times M}, \tag{7}$$

where $\mathbf{0}$ is a null column matrix with size $V+2$ and $\mathbf{0}^\sharp$ is a null matrix with the same shape of $\mathbf{R}^\sharp$ which is defined by

$$\mathbf{R}^\sharp = \begin{bmatrix} 1 & -1 & 0 & 0 & \cdots & 0 & 0 & 0 & 0 \\ 0 & 1 & -1 & 0 & \cdots & 0 & 0 & 0 & 0 \\ \vdots & \vdots & \vdots & \vdots & & \vdots & \vdots & \vdots & \vdots \\ 0 & 0 & 0 & 0 & \cdots & 1 & -1 & 0 & 0 \\ -1 & 0 & 0 & 0 & \cdots & 0 & 1 & 0 & 0 \end{bmatrix}_{V(L-1) \times (V+2)}; \tag{8}$$

(ii) Smoothness constraint on the adjacent radii of the vertically adjacent prisms. This constraint imposes that adjacent radii within vertically adjacent prisms must be close to each other. It forces the shape of all the estimated prisms to be similar. The matrix form of the this constraint is given by

$$\varphi_2(\mathbf{p}) = \mathbf{p}^\mathsf{T} \mathbf{R}_2^\mathsf{T} \mathbf{R}_2 \mathbf{p}, \tag{9}$$

where

$$\mathbf{R}_2 = \begin{bmatrix} \mathbf{R}_2^- & \mathbf{R}_2^+ & \mathbf{0}^* & \mathbf{0}^* & \cdots & \mathbf{0}^* & \mathbf{0}^* & \mathbf{0} \\ \mathbf{0}^* & \mathbf{R}_2^- & \mathbf{R}_2^+ & \mathbf{0}^* & \cdots & \mathbf{0}^* & \mathbf{0}^* & \mathbf{0} \\ \mathbf{0}^* & \mathbf{0}^* & \mathbf{0}^* & & & \vdots & \vdots & \vdots \\ \vdots & \vdots & \vdots & & & \vdots & \vdots & \vdots \\ \mathbf{0}^* & \mathbf{0}^* & \mathbf{0}^* & \cdots & \cdots & \mathbf{R}_2^- & \mathbf{R}_2^+ & \mathbf{0} \end{bmatrix}_{V(L-1) \times M}, \tag{10}$$

where $\mathbf{0}^*$ is a null matrix with the same shape of $\mathbf{R}_2^-$ and $\mathbf{R}_2^+$ which are defined by

$$\mathbf{R}_2^- = \begin{bmatrix} -1 & 0 & 0 & \cdots & 0 & 0 \\ 0 & -1 & 0 & \cdots & 0 & 0 \\ 0 & 0 & \ddots & & \vdots & \vdots \\ \vdots & \vdots & & \ddots & \vdots & \vdots \\ 0 & 0 & \cdots & 0 & -1 & 0 \end{bmatrix}_{V \times (V+2)} \tag{11}$$

and

$$\mathbf{R}_2^+ = \begin{bmatrix} 1 & 0 & 0 & \cdots & 0 & 0 \\ 0 & 1 & 0 & \cdots & 0 & 0 \\ 0 & 0 & \ddots & & \vdots & \vdots \\ \vdots & \vdots & & \ddots & \vdots & \vdots \\ 0 & 0 & \cdots & 0 & 1 & 0 \end{bmatrix}_{V\times(V+2)} \quad ; \tag{12}$$

(iii) The source's outcrop constraint. In the case of outcropping sources, this constraint imposes that the estimated horizontal cross-section of the shallowest prism must be close to the intersection of the geologic source with the known outcropping boundary. The matrix form of the this constraint is given by

$$\varphi_3(\mathbf{p}) = (\mathbf{A}\mathbf{p} - \mathbf{p}")^\mathsf{T} (\mathbf{A}\mathbf{p} - \mathbf{p}") , \tag{13}$$

where $\mathbf{p}"$ is a vector containing the parameters defining the polygon that represents the outcropping body given by

$$\mathbf{p}" = \begin{bmatrix} r_1^0 \\ r_2^0 \\ \vdots \\ r_M^0 \\ x_0^0 \\ y_0^0 \end{bmatrix}_{(V+2)\times 1} , \tag{14}$$

and

$$\mathbf{A} = \begin{bmatrix} \mathbf{I} & \hat{\mathbf{0}} \end{bmatrix}_{(V+2)\times M} , \tag{15}$$

where $\mathbf{I}$ is an identity matrix with shape $V+2$ and $\hat{\mathbf{0}}$ is null matrix with shape $M-(V+2)$;

(iv) The source's horizontal location constraint. In the case of outcropping sources, this constraint imposes that the estimated horizontal Cartesian coordinates of the arbitrary origin within the shallowest prism must be as close as possible to the known horizontal Cartesian coordinates of a point on the outcropping body. The matrix form of the this constraint is given by

$$\varphi_4(\mathbf{p}) = \left(\mathbf{B}\mathbf{p} - \mathbf{p}'\right)^\mathsf{T} \left(\mathbf{B}\mathbf{p} - \mathbf{p}'\right) , \tag{16}$$

where

$$\mathbf{B} = \begin{bmatrix} \mathbf{B}^\sharp & \hat{\mathbf{0}} \end{bmatrix}_{2\times M} , \tag{17}$$

$$\mathbf{B}^{\sharp} = \begin{bmatrix} 0 & \cdots & 0 & 1 & 0 \\ 0 & \cdots & 0 & 0 & 1 \end{bmatrix}_{2\times(V+2)}, \tag{18}$$

and $\mathbf{p}'$ is a vector containing the Cartesian coordinates of the horizontal location of the source given by

$$\mathbf{p}' = \begin{bmatrix} x_0^0 \\ y_0^0 \end{bmatrix}_{2\times 1}; \tag{19}$$

(v) Smoothness constraint on the horizontal position of the arbitrary origins of the vertically adjacent prisms. This constraint imposes that the estimated horizontal Cartesian coordinates of vertically adjacent prisms must be close to each other. It forces the estimated prisms to be approximately vertically aligned. The matrix form of the this constraint is given by

$$\varphi_5(\mathbf{p}) = \mathbf{p}^{\mathsf{T}}\mathbf{R}_5^{\mathsf{T}}\mathbf{R}_5\mathbf{p}, \tag{20}$$

where

$$\mathbf{R}_5 = \begin{bmatrix} \mathbf{R}_5^- & \mathbf{R}_5^+ & \mathbf{0}^{\pm} & \mathbf{0}^{\pm} & \cdots & \mathbf{0}^{\pm} & \mathbf{0}^{\pm} & \mathbf{0} \\ \mathbf{0}^{\pm} & \mathbf{R}_5^- & \mathbf{R}_5^+ & \mathbf{0}^{\pm} & \cdots & \mathbf{0}^{\pm} & \mathbf{0}^{\pm} & \mathbf{0} \\ \mathbf{0}^{\pm} & \mathbf{0}^{\pm} & \mathbf{0}^{\pm} & & & \vdots & \vdots & \vdots \\ \vdots & \vdots & \vdots & & & \vdots & \vdots & \vdots \\ \mathbf{0}^{\pm} & \mathbf{0}^{\pm} & \mathbf{0}^{\pm} & \cdots & \cdots & \mathbf{R}_5^- & \mathbf{R}_5^+ & \mathbf{0} \end{bmatrix}_{2(L-1)\times M}, \tag{21}$$

where $\mathbf{0}^{\pm}$ is a null matrix with the same shape of $\mathbf{R}_5^-$ and $\mathbf{R}_5^+$ which are given by

$$\mathbf{R}_5^- = \begin{bmatrix} 0 & 0 & \cdots & 0 & -1 & 0 \\ 0 & 0 & \cdots & 0 & 0 & -1 \end{bmatrix}_{2\times(V+2)}, \tag{22}$$

$$\mathbf{R}_5^+ = \begin{bmatrix} 0 & 0 & \cdots & 0 & 1 & 0 \\ 0 & 0 & \cdots & 0 & 0 & 1 \end{bmatrix}_{2\times(V+2)}; \tag{23}$$

(vi) Minimum Euclidean norm constraint on the adjacent radii within each vertical prism. This constraint imposes that all estimated radii within each prism must be close to null values. The matrix form of the this constraint is given by

$$\varphi_6(\mathbf{p}) = \mathbf{p}^{\mathsf{T}}\mathbf{C}^{\mathsf{T}}\mathbf{C}\mathbf{p}, \tag{24}$$

where

$$\mathbf{C} = \begin{bmatrix} \mathbf{C}^{\sharp} & \mathbf{0} & \mathbf{0} & \cdots & \mathbf{0} & \mathbf{0} \\ \mathbf{0} & \mathbf{C}^{\sharp} & \mathbf{0} & \cdots & \mathbf{0} & \mathbf{0} \\ \mathbf{0} & \mathbf{0} & \ddots & & \vdots & \vdots \\ \vdots & \vdots & & \ddots & \vdots & \vdots \\ \mathbf{0} & \mathbf{0} & \cdots & \cdots & \mathbf{C}^{\sharp} & \mathbf{0} \\ \mathbf{0} & \mathbf{0} & \cdots & \cdots & \mathbf{0} & 0 \end{bmatrix}_{M \times M}, \tag{25}$$

$$\mathbf{C}^{\sharp} = \begin{bmatrix} 1 & & & & \\ & \ddots & & & \\ & & 1 & & \\ & & & 0 & \\ & & & & 0 \end{bmatrix}_{(V+2)\times(V+2)}; \tag{26}$$

(vii) Minimum Euclidean norm constraint on the depth extent of all prisms. This constraint imposes that the estimated depth extent of the prisms must be close to a null value. The matrix form of the this constraint is given by

$$\varphi_7 = \mathbf{p}^{\mathsf{T}}\mathbf{D}^{\mathsf{T}}\mathbf{D}\mathbf{p}, \tag{27}$$

where

$$\mathbf{D} = \begin{bmatrix} 0 & \cdots & 0 \\ \vdots & \ddots & \vdots \\ 0 & \cdots & 1 \end{bmatrix}_{M \times M}. \tag{28}$$

Most of these constraints are defined by using the Tikhonov regularizing functions of order zero and one (Aster et al. 2019), by following the same approach presented by Oliveira Jr. et al. (2011). Here, we present the constraint on the depth extent of all prisms.

ACKNOWLEDGMENTS

REFERENCES

Aster, R. C., Borchers, B., & Thurber, C. H., 2019. *Parameter Estimation and Inverse Problems*, Elsevier, 3rd edn.

Barbosa, V. C. F., Silva, J. B. C., & Medeiros, W. E., 1999. Gravity inversion of a discontinuous relief stabilized by weighted smoothness constraints on depth, *Geophysics*, **64**(5), 1429–1437.

Dampney, C. N. G., 1969. The equivalent source technique, *Geophysics*, **34**(1), 39–53.

Emilia, D. A., 1973. Equivalent sources used as an analytic base for processing total magnetic field profiles, *Geophysics*, **38**(2), 339–348.

Junqueira-Brod, T. C., Roig, H. L., Caspar, J. C., Brod, J. A., & Meneses, P. R., 2002. A Província Alcalina de Goiás e a extensão do seu vulcanismo kamafugítico, *Revista Brasileira de Geociências*, **32**(4), 559–566.

Oliveira Jr., V. C. & Barbosa, V. C. F., 2013. 3-D radial gravity gradient inversion, *Geophysical Journal International*, **195**(2), 883–902.

Oliveira Jr., V. C., Barbosa, V. C. F., & Silva, J. B. C., 2011. Source geometry estimation using the mass excess criterion to constrain 3-D radial inversion of gravity data, *Geophysical Journal International*, **187**(2), 754–772.

Oliveira Jr., V. C., Sales, D., Barbosa, V. C. F., & Uieda, L., 2015. Estimation of the total magnetization direction of approximately spherical bodies, *Nonlinear Processes in Geophysics*, **22**(2).

Plouff, D., 1976. Gravity and magnetic fields of polygonal prisms and application to magnetic terrain corrections, *Geophysics*, **41**(4), 727–741.

Uieda, L., Oliveira Jr., V. C., & Barbosa, V. C. F., 2013. Modeling the earth with fatiando a terra, in *Proceedings of the 12th Python in Science Conference*, pp. 96 – 103.

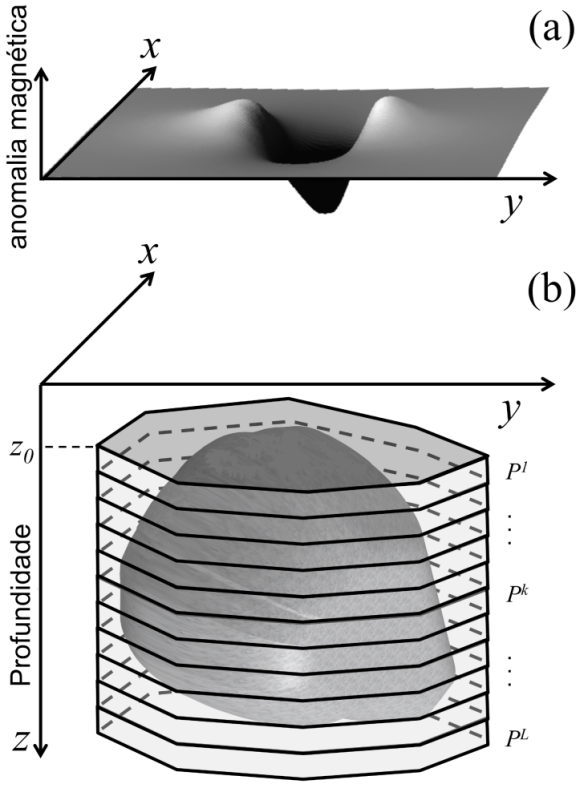

Figure 1. Schematic representation of (a) total-filed anomaly (grey surface) produced by (b) a 3-D anomalous source (dark grey volume). The interpretation model in (b) consists of a set of L vertical, juxtaposed 3-D prisms P^k , $k = 1, \ldots, L$, (light grey prisms) in the vertical direction of a right-handed coordinate system.

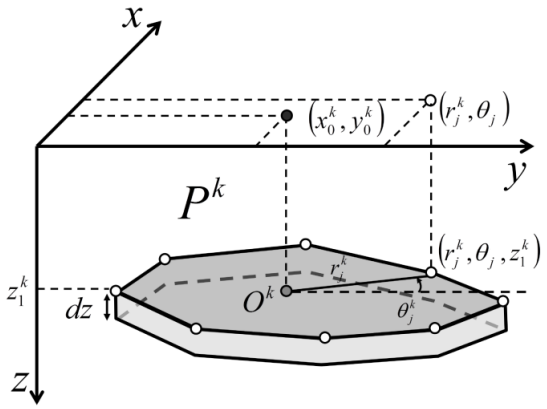

Figure 2. Polygonal cross-section of the kth vertical prism P^k described by V vertices (white dots) with polar coordinates (r_j^k , θ_j^k), $j = 1, \ldots, V$, $k = 1, \ldots, L$, referred to an arbitrary origin O^k (grey dot) with horizontal Cartesian coordinates (x_0^k , y_0^k), $k = 1, \ldots, L$, (black dot).

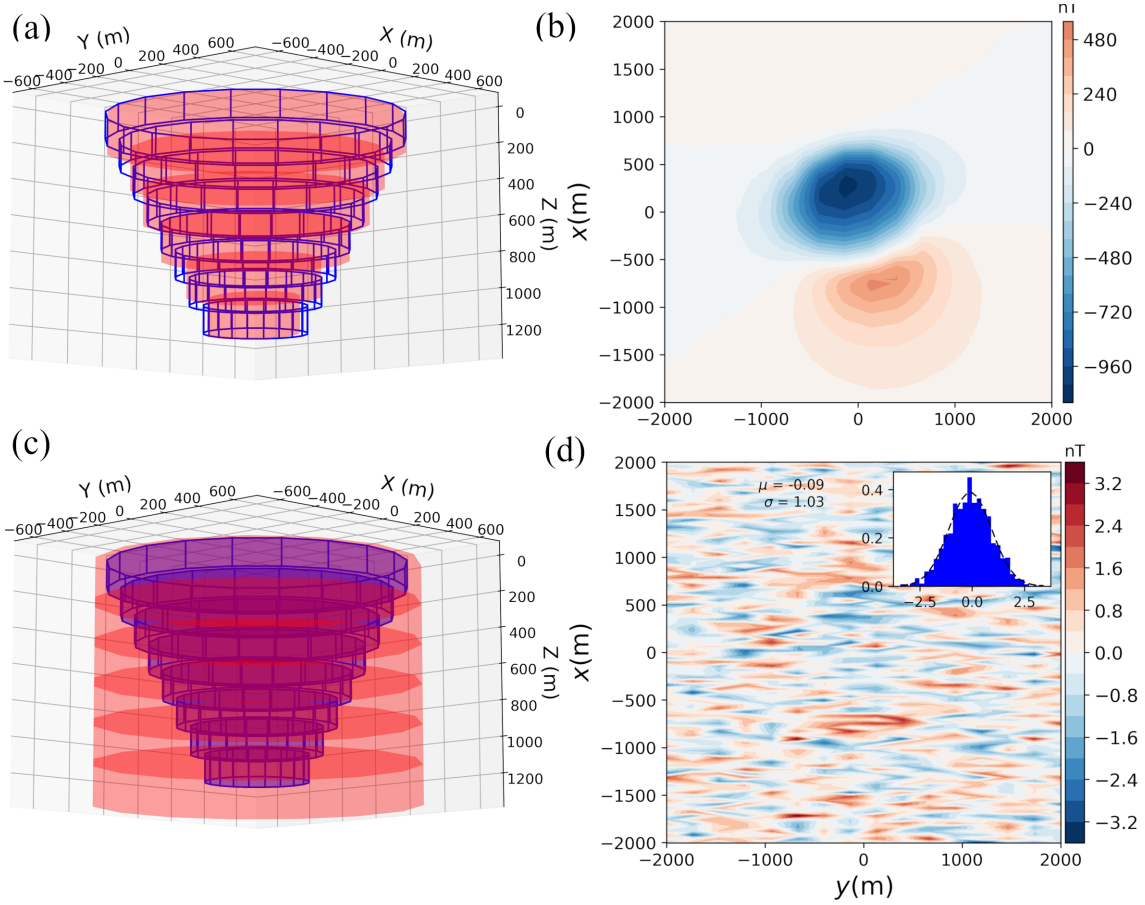

Figure 3. (a) Perspective view of the simple model with the depth to the top $z_0 = 50$ m and the depth extent 1200 m. (b) Synthetic noise-corrupted total-field anomaly produced by the simple model blue prisms in (a). The data was contaminated by a pseudorandom Gaussian noise with mean zero and standard deviation 1 nT. (c) Perspective view of the true (blue lines) and estimated body (red prisms) obtained by inverting the noise-corrupted total-field anomaly in (b). (d) Residuals defined as the difference between the noisy and the predicted (not shown) total-field anomalies; the latter was produced by the estimated body (red prisms in b). The inset in d shows the histogram and the Gaussian curve for the residuals with mean $\mu = 0.1$ nT and standard deviation $\sigma = 5.23$ nT.

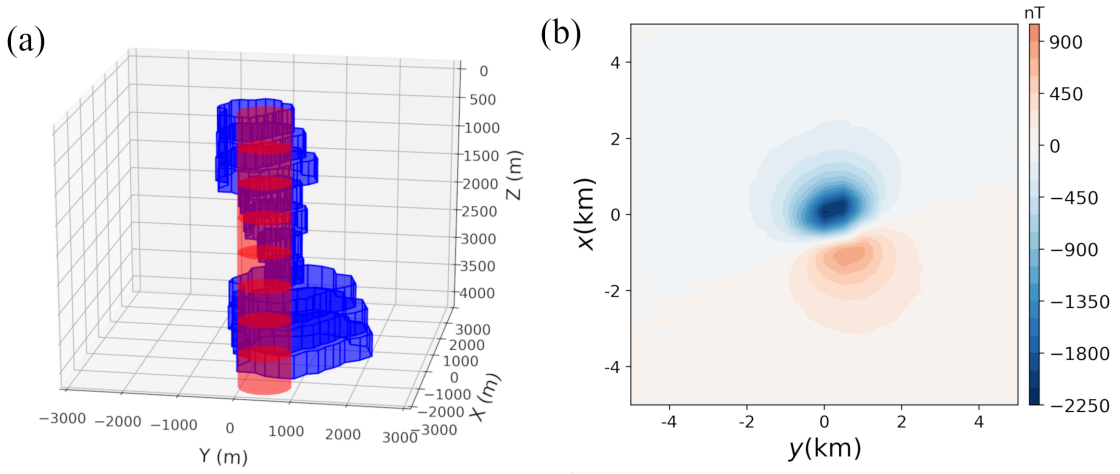

Figure 4. (a) Perspective view of the complex model (blue prisms) with the depth to the top $z_0 = 200$ m and the depth extent 4000 m and the initial guess (red prisms) for the inversion which is a cylinder with radius 500 m and depth extent 4800 m. (b) Synthetic noise-corrupted total-field anomaly produced by the complex model blue prisms in (a). The data was contaminated by a pseudorandom Gaussian noise with mean zero and standard deviation 5 nT.

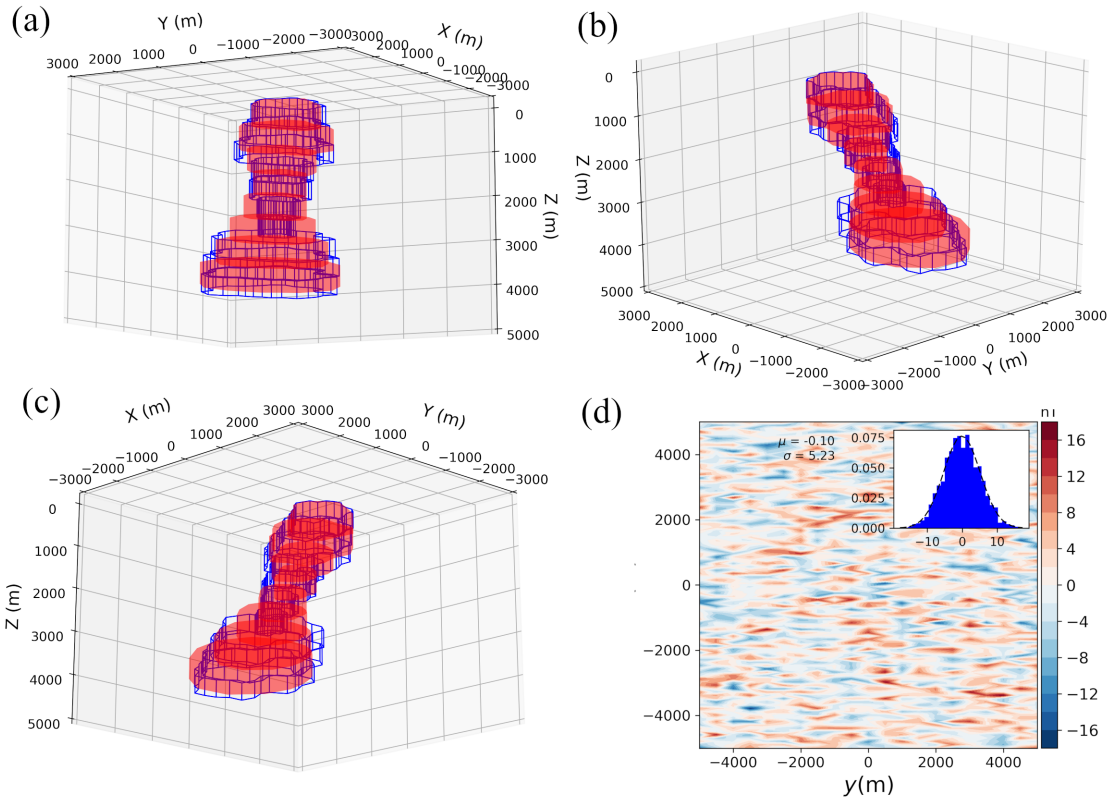

Figure 5. Perspective views of the complex model (blue lines) and the estimate (red prisms) in (a), (b) and (c). (d) Residuals defined as the difference between the noisy and the predicted (not shown) total-field anomalies and the histogram of the residuals (inset in d) with mean $\mu = 0.1$ nT and standard deviation $\sigma = 5.23$ nT. The dashed line on the inset is the Gaussian curve for the residuals.

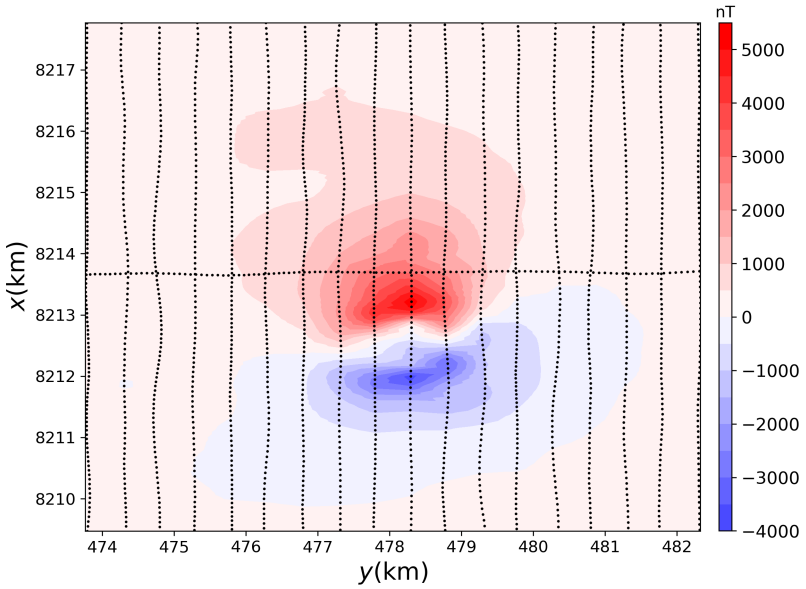

Figure 6. Total-field anomaly of Diorama in GAP. The black dots are the observation points used in this work.

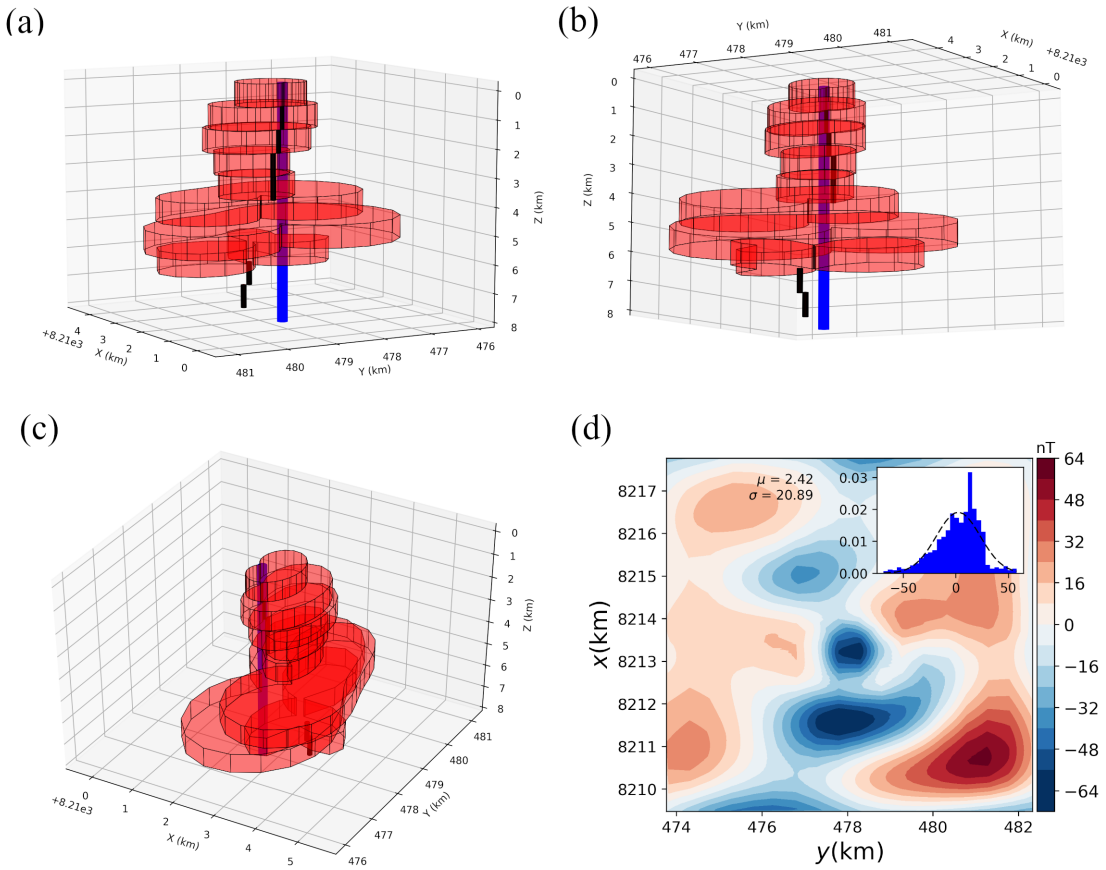

Figure 7. Perspective views of the initial guess (blue cylinder) and the estimated source (red prisms) in (a), (b) and (c). (d) Residuals defined as the difference between the noisy and the predicted (not shown) total-field anomalies and the histogram of the residuals (inset in d) with mean $\mu = 2.42$ nT and standard deviation $\sigma = 20.89$ nT. The dashed line on the inset is the Gaussian curve for the residuals.